VLE-based Phase Field Method to Simulate High-Pressure Diffuse Interface with Phase Change

Navneeth Srinivasan*, Hongyuan Zhang † and Suo Yang ‡
Department of Mechanical Engineering, University of Minnesota – Twin Cities, Minneapolis, MN 55455, USA

Supercritical fluids, often present in modern high-performance propulsion systems, result from elevated operating pressures. When these systems utilize fluid mixtures as fuel or oxidizers, a transcritical effect often occurs. This effect can lead to misjudgments, as mixture critical points exceed those of individual components. Fluid mixing may induce phase separation, creating liquid and vapor phases due to the transcritical multi-component effect. Consequently, two-phase modeling is essential for transcritical and supercritical fluids. Traditional interface capturing methods, like Volume of Fluid (VOF) and Level Set (LS), present challenges such as computational expense and lack of conservatism. The Phase Field (PF) method, or the Diffuse Interface (DI) method which uses a phase fraction transport equation, emerges as a conservative alternative. Despite the absence of an initial interface in transcritical fluids, phase separation from mixing may form liquid droplets, necessitating multiphase modeling. To address these complexities, a Vapor-Liquid Equilibrium (VLE) model, coupled with the PR equation of state, is introduced. This model estimates phase fractions, liquid and vapor compositions, densities, and enthalpies through a flash problem solution. The conventional PF model is enhanced by replacing the phase fraction transport equation with VLE-derived values. The resulting VLE-based PF method is implemented into an OpenFOAM compressible solver, ensuring numerical stability with explicit phase field terms and a new CFL criterion. Test cases involve 1D interface convection and 2D droplet convection. In the 1D test, the VLE-based PF model adeptly captures interfaces, adjusting thickness as needed. The 2D droplet case, challenging due to a non-aligned Cartesian grid, exhibits uniform interface thickness and preserves droplet shape. The VLE-based PF model demonstrates versatility and reliability in capturing complex fluid behaviors, offering promising prospects for future research.

I. Introduction

With ever increasing demand for high performance combustors, increasing the chamber pressure is one often sought-after option. This leads to the working conditions to overlap with the supercritical regime of the reactants. Due to the high-pressure environment in engine combustors, the injected multi-component liquid propellants and fuel-air mixtures often go through thermodynamically transcritical processes during the spray breakup, evaporation, mixing, and combustion processes. Efficient spray breakup and evaporation of liquid fuels are the primary targets of engine combustor design and control to ensure sufficiently small "effective" evaporation time. The existing liquid fuel injectors and multi-component liquid fuels developed for low pressures are not optimal at high pressures, and hence require redesign and optimization.

To understand the subcritical and supercritical injection, mixing, and combustion process, high-fidelity simulation tools are needed. Since supercritical region is far from the ideal gas region, real-gas effect needs to be considered to capture correct behavior. In addition, transcritical and supercritical fluid behavior can be peculiar because of the large variation of thermophysical properties such as density and specific heat near the critical point. As a result, the Computational Fluid Dynamics (CFD) modeling of supercritical flows is very challenging. Since small changes in temperature and pressure can have large effects on the structure of a fluid near the critical point, local properties are very important. Furthermore, a supercritical fluid lacks surface tension, which means the modeling transcritical flow needs to capture the surface tension change when the fluid goes across phase boundary. This makes simulation of transcritical flows more challenging than supercritical flows.

^{*}Ph.D. Student, srini237@umn.edu, Student Member AIAA.

[†]Ph.D. Candidate, zhan6305@umn.edu, Student Member AIAA.

[‡]Richard & Barbara Nelson Assistant Professor, suo-yang@umn.edu (Corresponding Author), Senior Member AIAA.

The studies of transcritical and supercritical injection, mixing, and combustion have attracted much interest in the past 30 years. However, most of them were mainly concentrated on the single-component system, whose critical point is a constant value. As long as the fluid exceeds its critical point, it goes into the supercritical state, and the classical "dense-fluid" approach is used with the assumption of a single-phase [1]. Since the real mixture critical pressure could be significantly higher than the critical pressure of each component [2], the accurate mixture critical point needs to be obtained.

Our previous work by Zhang & Yang [3] [4] and Srinivasan et al. [5] showed the complex phenomena associated with transcritical phase change in different configurations, such as shock-droplet interaction and temporal mixing layers. The presence of two phase regions as well as phase separation in these systems were captured by these works. As a limitation of the Navier-Stokes Equations, a sharp interface (e.g., at low pressures) is not permitted as the derivatives are not defined there. This requires initial conditions with diffused interface to ensure no sharp gradient is present in the system, which can lead to spurious oscillations and even divergence. On the other hand, high-pressure supercritical and transcritical interfaces are expected to be thickened, and the usage of diffused interface initialization might be acceptable; however, using any CFD code, numerical diffusion will further increase the interface thickness, resulting in complete smearing which is not physical. Hence, these interface regions require special treatment in order to regulate the impact of numerical diffusion.

Traditionally, multiphase problems at low pressures are tackled by two main approaches - interface tracking and interface capturing methods. The latter is preferred over the former, due to its ability to capture dynamically morphing interfaces. The interface capturing methods can further be classified into volume of fluid (VOF), level set (LS), and phase field (PF) methods. The VOF method involves a complex and expensive interface reconstruction step and the LS method is not conservative. The PF method introduces a new way for interface capturing, which can be made conservative and simple, called the diffuse interface method. Jain et al. $\boxed{0}$ introduced an accurate and conservative PF method for low-pressure compressible multiphase flow systems. This method is built upon the work of Chiu and Lin $\boxed{0}$, who used the Allen-Cahn equation to develop the PF model for incompressible flow. The common idea behind these methods is the usage of a phase tracking variable - phase fraction ϕ , deriving a transport equation for ϕ to define the two phase system, and finally adding the phase fraction interface regulation term accordingly. This regulation term allows both the smearing as well as shrinking of the interface, and can be tuned by the user-defined interface thickness term (e.g., if the physical interface thickness is known). The phase fraction regulation impacts the interface physics and is expected to impact all the variables present in the system as well. Thus, the regulation term-based flux is also added to conservative equations (mass, momentum, energy, species) to ensure any interface correction is appropriately accounted for in all the variables.

The importance of the usage of PF method has been clearly motivated in previous works for low-pressure multiphase flows, but its applicability to high-pressure transcritical fluids is yet to be studied. PF methods with phase change have been used for applications such as solid-gas interfaces as well as low-pressure incompressible liquid-vapor interfaces, but usually employ the vapor pressure and saturation pressure methodology for evaporation/condensation (i.e., phase change) flux estimation. However, for high-pressure transcritical fluids, phase change and phase separation need not occur purely due to evaporation at the interface but can also occur due to the multi-component mixing effect and micro-explosion within the liquid phase. The vapor-liquid equilibrium (VLE) theory has been successfully used to capture phase change as well as phase separation by our previous works [3-5]. The VLE solution provides the phase fraction along with other information such as phase compositions and phase densities.

In this study, we attempt to replace the phase field transport equation with the VLE solution to obtain the phase field and then correct all the conservative equations accordingly. Our VLE framework coupled with a fully compressible solver will be modified to incorporate the new phase field regulation terms into the conservation equations. Simple cases such as interface thickening and droplet convection cases will be tested first, followed by a turbulent temporal mixing layer (TML) case with interface thickening.

II. Numerical Methods

A. Models of thermodynamic and transport properties

Here, we use VLE solvers to capture the phase change and determine the critical point of multi-component mixture in high-pressure transcritical multiphase flows as described above. VLE describes the phase equilibrium between liquid and vapor phases by solving a set of VLE equations to give the phase fraction and compositions in the two phases. If the gas (vapor) phase mole fraction is equal to 0 or 1, then the system is in a purely liquid or gaseous phase, respectively. If

the system falls into the two-phase region, gas phase mole fraction will be between 0 and 1, and an equilibrium between vapor and liquid will be observed. If at certain conditions, thermodynamic properties become identical between liquid and gas, it indicates the occurrence of transcritical transition from a subcritical state to a supercritical state (which could be either a liquid-like or gas-like state).

The CFD solver is coupled with isobaric and isenthalpic (PHn) flash solver [9]. PHn flash and almost all other VLE solvers, are developed based on Temperature-Pressure-molefraction (TPn) flash. Specifically, PHn flash solves the VLE equation set at given enthalpy (H) rather than temperature (T). TPn flash is the most basic VLE solver, which solves a set of VLE equations at given temperature (T), pressure (P), and mole fraction of each component (n) in the system.

Isothermal and isobaric (TPn) flash: VLE is governed by fugacity equality Eq. (1) and Rachford-Rice equation [10] Eq. (2), which is an additional constraint to the equilibrium solver as used in Saha and Carroll [11] and obtained from the conservation of each component.

$$f_{i,l}/f_{i,g} = 1, (1)$$

$$\sum_{i=1}^{N} \left\{ z_i \left(1 - K_i \right) / \left[1 + \left(K_i - 1 \right) \phi_v \right] \right\} = 0, \tag{2}$$

$$K_i = y_i / x_i, (3)$$

$$\sum_{i=1}^{N} x_i = \sum_{i=1}^{N} y_i = 1,\tag{4}$$

where $f_{i,p}$ is the fugacity of component i in phase p (p = l: liquid; p = g: gas), x_i is the mole fraction of component i in liquid phase, y_i is the mole fraction of component i in gas phase, z_i is the mole fraction of component i in the feed (i.e., the entire mixture including both gas phase and liquid phase), ϕ_v is the gas mole fraction, K_i is the equilibrium constant of component i.

The real fluid properties are described using the Peng-Robinson equation of state (PR-EOS) [12] as:

$$P = \frac{RT}{V - b} - \frac{a}{V(V + b) + b(V - b)},$$
(5)

where P, R, T and V are pressure, gas constant, temperature, and specific volume, respectively. For a single-component fluid, the PR-EOS parameters are given by

$$a = 0.45724 \frac{R^2 T_c^2}{p_c} \hat{a},$$
 $b = 0.07780 \frac{RT_c}{p_c},$ (6)

$$\hat{a} = \left(1 + \kappa \left(1 - (T_r)^{1/2}\right)\right)^2, \qquad \kappa = 0.37464 + 1.54226\omega - 0.26992\omega^2, \tag{7}$$

where subscript "c" means critical value, subscript "r" means the reduced value (e.g., $T_r = T/T_c$), and ω is the acentric factor.

The liquid phase and the gas phase are described by two multi-component PR-EOS, respectively. The specific volume of each phase, V_p , is solved from the respective PR-EOS. The compressibility factor of each phase (Z = PV/RT) can also be obtained from this.

The fugacity formula of PR-EOS is shown below [13]:

$$f_{i} = P\chi_{i} \exp\left[\frac{B_{i}}{B_{mix}}(Z-1) - ln(Z-B_{mix}) - \frac{A_{mix}}{2\sqrt{2}B_{mix}} \left(\frac{2\sum_{j}x_{j}A_{j}}{A_{mix}} - \frac{B_{i}}{B_{mix}}\right) ln\left(\frac{Z+(1+\sqrt{2})B_{mix}}{Z+(1-\sqrt{2})B_{mix}}\right)\right], \quad (8)$$

where χ_i is the mole fraction of component i (for liquid, $\chi_i = x_i$; for gas phase, $\chi_i = y_i$),

$$A_i = \frac{a_i p}{R^2 T^2},\tag{9}$$

$$B_i = \frac{b_i p}{RT},\tag{10}$$

$$A_{mix} = \sum_{i} \sum_{j} x_{i} x_{j} (1 - b_{ij}) \sqrt{A_{i} A_{j}},$$
(11)

$$B_{mix} = \sum_{i} x_i B_i. \tag{12}$$

The equation set Eq. (1-12) is solved based on Newton iteration method. The flow chart of the TPn flash is shown in Fig. [1]. The initial guess is obtained using the Wilson Equation [14]:

$$K_i = e^{5.373(1+\omega_i)(1-1/T_{r,i})}/P_{r,i},$$
(13)

where ω_i is the acentric factor of component i; $T_{r,i}$ and $P_{r,i}$ are the reduced temperature and reduced pressure of component i, respectively.

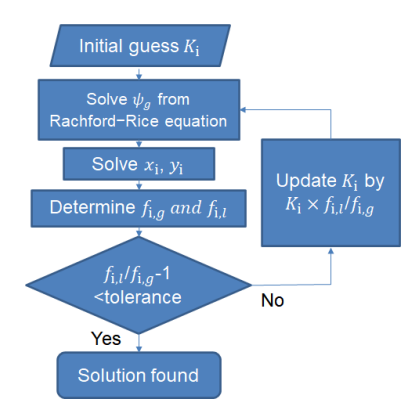


Fig. 1 Flow chart of the TPn flash solver.

PV flash and UV flash: The PV flash and UV flash solvers are developed based on the TP flash. Both of them use iteration methods. Specifically, initial guesses (T for PV flash; T and P for UV flash) are obtained from the previous time step, and a TP flash problem is solved in each iteration. After several iterations, when the error is smaller than tolerance, the solver returns a solution.

In PV flash, since pressure (P) is already given as an input, only temperature (T) needs to be guessed and updated during the iteration. A secant method is used to avoid the expensive derivative computation in the Newton-Raphson method. In UV flash, two variables (both T and P) need to be guessed and updated simultaneously during the iteration, and hence the secant method cannot be applied. The Newton-Raphson method is used to solve the UV flash problems. The required Jacobian matrix is obtained using the analytical framework of Tudisco and Menon [15].

Transport properties: The dense fluid formula (i.e., Chung's method) [16] is used to evaluate the dynamic viscosity and thermal conductivity under transcritical conditions. This method gives accurate estimations of viscosity and thermal conductivity of polar, non-polar and associating pure fluids and mixtures. Its dynamic viscosity and thermal conductivity have a similar formula:

$$\lambda = \lambda_0 \lambda^* + \lambda_p,\tag{14}$$

where λ represents dynamic viscosity or thermal conductivity. λ_0 is the gas property at low pressures. λ^* and λ_p are high-pressure corrections. At high pressures, λ_p is the major contributing term comparing to $\lambda_0\lambda^*$. On the other hand, at low pressures, λ^* is approaching unity, and the λ_p term is negligible such that Eq. 14 reduces to λ_0 . Hence, the transition between subcritical and supercritical is smoothly described by the model. For mass diffusivity, we used mixture-averaged mass diffusion model. The mass diffusion coefficient of specie i, D_i is defined by Kee et al. 17:

$$D_{i} = \frac{1 - Y_{i}}{\sum_{j \neq i}^{N} X_{j} / D_{j,i}},$$
(15)

where Y_i and X_i are the mass and mole fractions of the i-th component, respectively; $D_{i,j}$ is the binary diffusion coefficient, which is evaluated by Fuller's model [18] with Takahashi's correction for high pressures [19].

B. Phase Field Based Compressible Flow Solver Formulation

The equation of mass, momentum (neglecting body force), and total energy conservation, together with species transport with the inclusion of the phase field regulation term can be written as:

$$\frac{\partial \rho}{\partial t} + \nabla \cdot (\rho u) = \nabla \cdot ((\rho_l - \rho_v) \overrightarrow{a_l}), \tag{16}$$

$$\frac{\partial \rho u}{\partial t} + \nabla \cdot (\rho u \otimes u) = -\nabla p + \nabla \cdot \tau + \nabla \cdot (\overrightarrow{f} \otimes u) + \sigma \kappa \nabla \phi_l, \tag{17}$$

$$\frac{\partial \rho Y_s}{\partial t} + \nabla \cdot (\rho Y_s u) = -\nabla \cdot j_s + \nabla \cdot \overrightarrow{R_s}, \qquad s = 1, ..., n_s$$
 (18)

$$\frac{\partial \rho E}{\partial t} + \nabla \cdot (\rho E u) = -\nabla \cdot (u p) + \nabla \cdot (u \cdot \tau) + \nabla \cdot q + \nabla \cdot (\overrightarrow{f} u^2) + \nabla \cdot (\Sigma_s \overrightarrow{R_s} h_s) + \sigma \kappa u, \qquad s = 1, ..., n_s$$
 (19)

where ρ is the mixture density, p is the pressure, u is the velocity, τ is the viscous stress tensor, q is the heat flux, $E = e + \frac{1}{2}u \cdot u$ is the total energy. In Eq. (18), Y_s and j_s are the mass fraction and mass diffusion flux respectively, while n_s is the total number of species.

The additional components embedded within the conservation equations are attributed to the phase field regulation. The inclusion of phase field regulation terms in the governing equations serves the purpose of rectifying the values associated with all conserved variables when implementing the phase field method at the interface. These terms adhere to the formulation introduced by Jain et al. [6, 7]. Notably, a key departure in the current methodology from the approach proposed by Jain et al. [6, 7] lies in the exclusion of the phase fraction transport equation. Instead, the phase fraction (ϕ_v) is derived from the solution of the VLE equations, serving as the means to delineate the interface.

The source term for mass regulation serves the purpose of controlling the fluid density across the interface, utilizing the densities of the liquid phase (ρ_l) and gas phase (ρ_v) . The conservative form of the momentum phase regulation term is introduced to mitigate spurious oscillations, a strategy akin to that employed by Jain et al. [7]. Furthermore, the momentum equation incorporates a surface tension source term, where σ represents the surface tension coefficient and κ signifies the curvature of the interface. The correction term for the species transport phase field is imperative for rectifying the mass fractions of species across the interface. In the context of the energy equation, two correction terms are incorporated: one pertaining to the kinetic energy of the velocity correction flux and the other associated with the enthalpy transport resulting from the species flux correction. Additionally, the energy equation includes a surface energy term.

The phase field regulation terms included in the above conservative equations have the following form:

$$\phi_l = 1 - \phi_v \tag{20}$$

$$\overrightarrow{a_l} = \Gamma[\epsilon \nabla \phi_l - \phi_l (1 - \phi_l) \frac{\nabla \phi_l}{|\nabla \phi_l|}], \tag{21}$$

where ϕ_l is the liquid phase fraction and flux velocity, $\Gamma = max(u)$ and interface thickness $\epsilon = \lambda \Delta x$, where Δx is the grid spacing and λ is the number of grid points required across the interface ($\lambda = 1$ unless mentioned otherwise).

$$\overrightarrow{a_{v}} = -\overrightarrow{a_{l}} \tag{22}$$

$$\overrightarrow{f} = (\rho_l - \rho_v)\overrightarrow{a_l} \tag{23}$$

$$\overrightarrow{R_s} = (\rho_l Y_{s,l} - \rho_v Y_{s,v}) \overrightarrow{a_l}$$
 (24)

The regulation terms outlined above necessitate the determination of phase fraction, along with the densities and compositions of the phases. This determination is accomplished through the previously established VLE framework, eliminating the need to solve a separate transport equation for the phase fraction.

C. Numerical Implementation of Phase Field Terms

The phase field, characterized by compressible governing equations, has been integrated into the OpenFOAM compressible CFD solver, specifically, the rhoCentralFoam solver [20]. Within the OpenFOAM framework, this open-source solver operates as a single-component, fully compressible and conservative, ideal gas equation of state-based CFD solver. It employs the central upwind scheme [21] for discretizing convection terms and utilizes a unity Lewis number approximation for transport. The code has been modified to accommodate multiple species and implement

mixture-averaged transport, as detailed by Zhou et al. [22]. Additionally, this modified solver incorporates a high-pressure VLE model, which accounts for non-ideal transport and departure functions to estimate thermodynamic properties, as presented by Zhang et al. [4, 23].

The incorporation of phase field regulation terms into the governing equations involves discretization through the central upwind-based flux splitting method utilized by OpenFOAM. In this process, all field variables are interpolated onto cell faces, and phase field regulation flux terms are then estimated on the cell face for each governing equation. Face field reconstruction is carried out using the van Leer limiter [24]. Spatial discretization is consistently maintained at a second-order level, and Euler time integration is employed. The phase field terms are formulated as explicit terms, necessitating the incorporation of their stability into the Courant-Friedrichs-Lewy (CFL) number for simulation stability.

Adapting from Jain et al. [6], the CFL number (CFL_{PF}) associated with the phase field terms can be written as:

$$CFL_{PF} = \frac{6\Gamma\epsilon\Delta t}{(\Delta x)^2} \tag{25}$$

Where, Δt is the time step and Δx is the cell spacing. The above defined CFL is applicable for 3D simulations with a fixed cell size, which can be easily generalized to varying grid sizes by replacing Δx by $v_{cell}^{1/3}$. If 2D or 1D simulations are performed, then the CFL number (CFL_{PF}) can be modified by replacing the 6 in the numerator with 4 and 2 respectively.

The flow based CFL number is defined as:

$$CFL_{flow} = \frac{|U|_{max}\Delta t}{\Delta x} \tag{26}$$

In order to ensure the flow simulation is numerically stable, both the flow CFL and phase field CFL are combined as shown below:

$$CFL = max\left(\frac{6\Gamma\epsilon}{(\Delta x)^2}, \frac{|U|_{max}}{\Delta x}\right)\Delta t$$
 (27)

This new CFL definition has been incorporated into the compressible flow solver and CFL for all simulations has been set to 0.1.

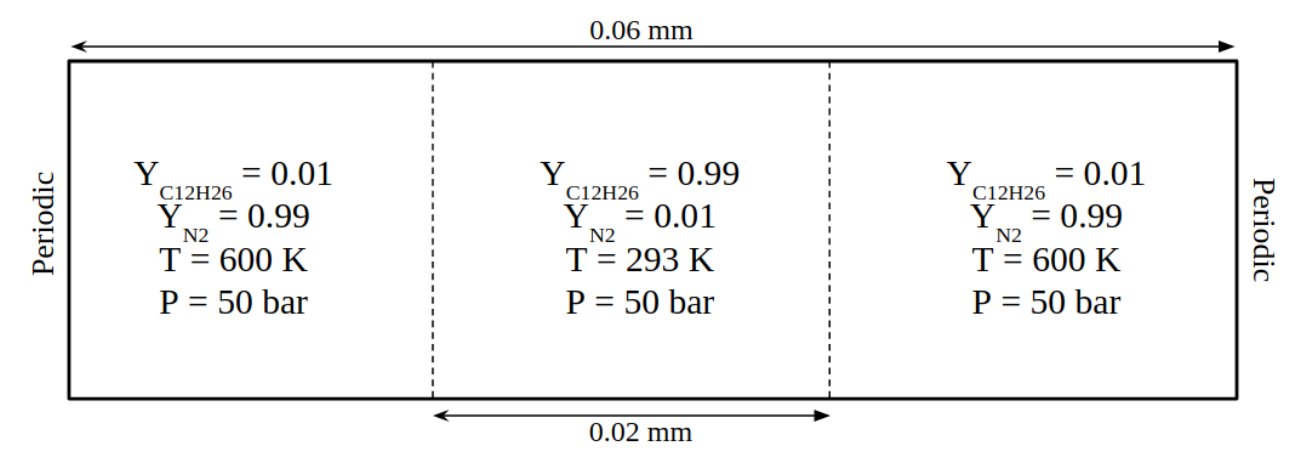


Fig. 2 Domain and configuration for 1D interface convection test. (384 grid points)

III. Results

A. 1D Interface Convection

The initial test case for the VLE based phase field method involves a one-dimensional interface convection scenario. The domain and configuration for this test case are depicted in Figure $\boxed{2}$. The periodic domain spans a length of 0.06 mm and is discretized into 384 equally spaced points. Within a segment of length 0.02 mm, $C_{12}H_{26}$ is initialized at 293 K, while the surrounding regions consist of N_2 at 600 K. The system operates at a pressure of 50 bar, and an initial

velocity of 100 m/s (1D velocity) is prescribed. Despite the expectation that the system would exhibit purely convective behavior, treating all variables as passive scalars, the governing equations outlined in Section [II.B] are all solved in 1D retaining all the physics.

This test case is designed to elucidate the influence of phase field-based interface regulation and to assess the ramifications of incorporating the new terms into the governing equations.

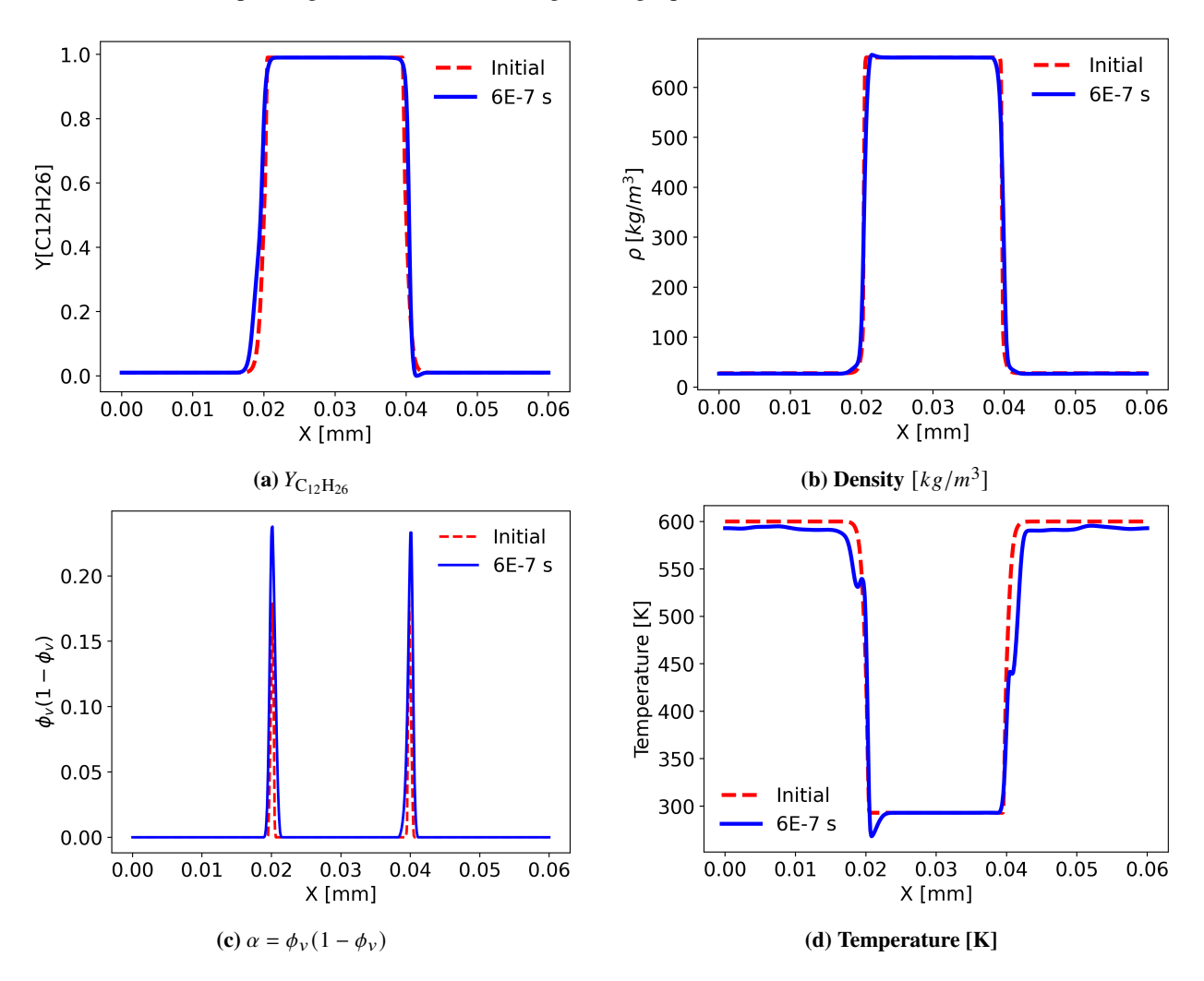


Fig. 3 1D convection test results comparison of initial field with field at time t = 6E - 7s (1 flow through time)

Figure 3 presents a comparison of all fields after one flow-through time. It is assumed that the impact of the phase field regulation terms has reached a steady state after this duration for the 1D test case. As depicted in Figure 3a, the mass fraction of $C_{12}H_{26}$ exhibits a close agreement with the initial field. The effect of the phase field terms on fluid density is illustrated in Figure 3b, where both the interface densities and thickness seem to be preserved even after one flow-through time.

To enhance the clarity of visualizing the interface, the utilization of $\alpha = \phi_v (1 - \phi_v)$ is deemed a more effective metric compared to ϕ_v or ϕ_l . This metric has been previously employed in the literature ([3-5] [23]) for visualizing and tracking the interface. It's worth noting that α is expected to have a maximum value of 0.25, occurring when $\phi_v = \phi_l = 0.5$. In the 1D case, as illustrated in Figure [3c] it might appear that the interface is thickening, given that the initial field seems narrower compared to the field after one flow-through time. However, the increase in peak values indicates that the phase field regulation terms are compelling the interface ($\alpha = 0.25$) to exist precisely at one grid point ($\lambda = 1$, as referenced in Section [II.B]). This observation underscores the capability of the phase field regulation method to adjust the interface from sharper initial conditions to more diffused interfaces or vice versa.

The temperature field comparison is depicted in Figure 3d, revealing the presence of noticeable oscillations. Such

oscillations are commonly encountered in compressible flow simulations, particularly when employing real fluid equations of state such as the PR-EOS, as illustrated by Zhang et al. [23]. However, the focus of interest in this comparison lies in the interface region, where the phase field regulation terms are active. It is observable that the regulation terms effectively maintain the temperature along the interface, and the $C_{12}H_{26}$ rich region temperature aligns well with the initial conditions.

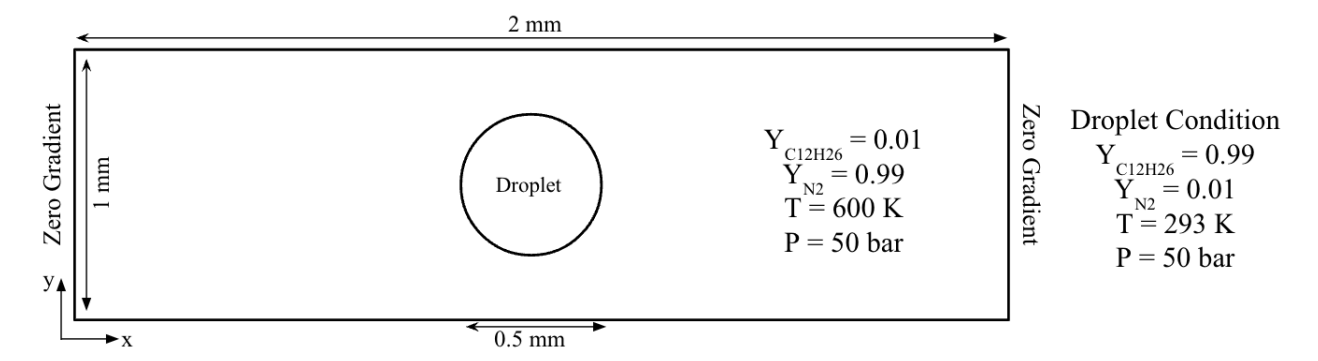


Fig. 4 Domain and configuration for 2D droplet convection test. $(512 \times 256 \text{ grid points})$

B. 2D Droplet Convection

The preceding section and results were centered on the 1D convection of the interface. In this section, we extend our investigation to assess the impact of phase field regulation in a 2D system. Specifically, we consider a droplet convection case to evaluate the performance of the VLE based phase field regulation terms. The domain and configuration of this case are detailed in Figure 4. The domain for this study is a 2 mm long and 1 mm wide region, discretized into 512 in x direction and 256 points in the y direction. All boundaries are configured as zero-gradient outlet faces. The bulk flow is initially enriched with N_2 at a temperature of 600 K. In the middle of the domain, a droplet with a diameter of 0.5 mm is initialized. The droplet is rich in $C_{12}H_{26}$ and initialized at a temperature of 293 K. The system operates at a pressure of 50 bar, and a uniform velocity of 100 m/s along the x-direction is imposed. All governing equations are solved in 2D for this case. Although surface tension has been included in the governing equations, it has been deactivated for this particular test case.

This test case is particularly intriguing because the grid has been structured as a uniform Cartesian mesh, which does not align with the droplet interface (unlike the 1D test case). The comparison between the initial condition for the 2D droplet convection case and the flow field after a time $t = 4 \times 10^{-7}$ s (referred to as the final time for this discussion) is presented in Figure [5].

Figure 5a illustrates the initial condition for the species mass fraction of $C_{12}H_{26}$, while Figure 5b shows the contour of the mass fraction at the final time. The phase field regulation term appears to perform admirably in regulating the droplet shape, as well as the mass fractions across the interface, even for the 2D case. Density contours for the initial and final times are displayed in Figure 5c and Figure 5d respectively. Similar to the mass fraction, density contours exhibit effective regulation across the interface while maintaining the droplet shape throughout the convection process.

Here, $\alpha = \phi_v(1 - \phi_v)$ serves as the interface indicator, as in the previous test case. The interface thickness and shape have been well retained by the phase field method throughout the convection flow time, even for the 2D droplet case. Finally, temperature contours are compared between the two times in Figures $\boxed{5g}$ and $\boxed{5h}$. At the final time, it may appear that the temperature interface is growing thicker than the initial condition. This is associated with the convection of species enthalpies from the initial condition provided at the interface, representing an intermediate temperature compared to the droplet and bulk.

In summary, the VLE based phase field method demonstrates excellent performance in the 2D droplet test case.

IV. Conclusions and Future Work

Supercritical fluids are prevalent in modern high-performance propulsion systems, primarily attributed to increased operating pressures. Often, these systems employ multicomponent mixtures as either fuel or oxidizers, inducing the transcritical effect. Notably, critical points of mixtures surpass those of individual components, potentially leading to

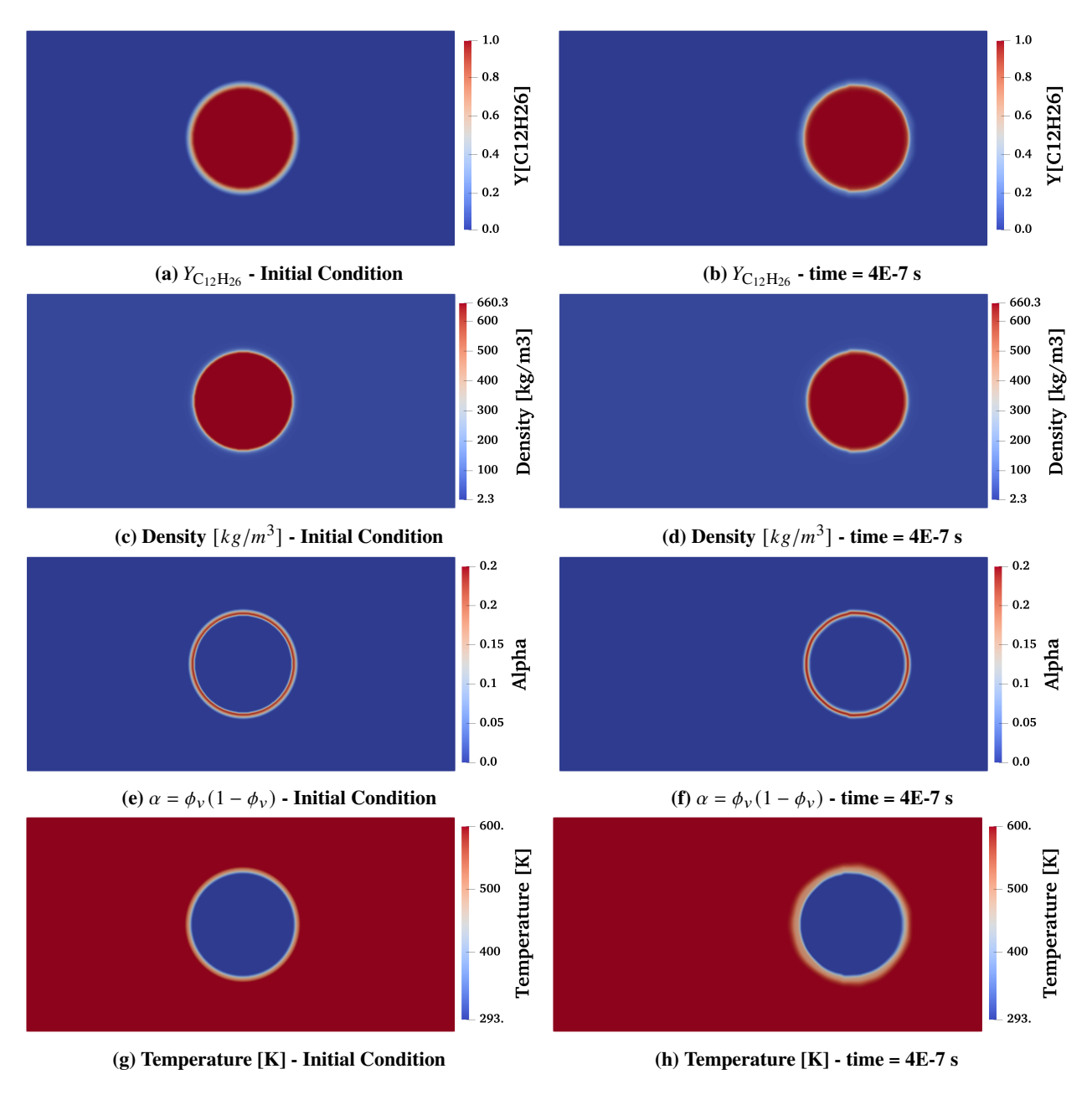


Fig. 5 2D droplet convection test results comparison of initial fields with fields at time t = 4E-7 s

the misclassification of subcritical fluids as supercritical. Moreover, fluid mixing may prompt phase separation, yielding liquid and vapor phases due to the transcritical multi-component effect. Consequently, the imperative for two-phase modeling arises in the context of transcritical and supercritical fluids. Traditional interface capturing methodologies, such as Volume of Fluid (VOF), entail a computationally expensive interface reconstruction step, exacerbating the already substantial computational costs associated with transcritical flow simulations. Conversely, the Level Set (LS) method lacks conservatism. The Phase Field (PF) method, also recognized as the Diffuse Interface (DI) method, presents a conservative and easily integrated approach with flow equations. Generally, the DI method involves solving a transport equation for the phase fraction in conjunction with other governing equations, introducing interface regulation terms to govern interface thickness. However, in instances involving transcritical fluids, even if the initial conditions do not contain two phase mixtures, phase separation from mixing can yield liquid droplets, necessitating multiphase modeling. To calculate the thermophysical states and vapor fractions for transcritical mixtures, the Vapor Liquid Equilibrium

(VLE) model, coupled with the Peng Robinson equation of state, is employed. The VLE model determines the phase fraction of a given mixture through the resolution of a flash problem, yielding critical insights into liquid and vapor composition, phase fraction, liquid and vapor densities, as well as enthalpies and energies.

In this study, the conventional phase fraction transport equation in the original PF formulation is replaced with the phase fraction derived from VLE calculations. Subsequently, the development and integration of phase field regulation terms into the governing equations are undertaken. This innovative VLE-based phase field method is incorporated into a conservative compressible CFD solver implemented on the OpenFOAM platform, accounting for non-ideal transport. The estimation of phase field regulation fluxes involves the reconstruction of cell center values onto faces, followed by the estimation of fluxes on these faces. The phase field terms are introduced explicitly, and a new CFL criterion is introduced to ensure numerical stability.

The VLE based PF model is tested for two configurations: a 1D interface convection and a 2D droplet convection test case. All governing equations are solved for both scenarios. In the 1D test case, the phase field regulation demonstrates excellent interface capturing while also ensuring the accurate reconstruction of conserved flow variables across the interface through regulation. Despite the initial condition featuring a sharp interface, the phase field regulation effectively adjusts the interface thickness to exist at the user-specified width mentioned. This showcases the adaptability of the VLE-based phase field method to even grow the interface thickness if required. Moving to the 2D droplet convection case, a standard test case for multiphase model development, the VLE-based PF model exhibits commendable performance. The interface thickness remains consistently uniform, and no significant distortion to the droplet shape is observed. Notably, this test case holds particular significance as a uniform Cartesian grid, which does not align with the droplet's interface, is employed. The VLE-based PF model demonstrates robust performance even under these conditions.

Subsequent research for this model entails assessing interface regulation in more demanding scenarios, including a droplet in a shearing flow and droplets in homogeneous isotropic turbulence. Additionally, the future investigation will also explore the impact of high temperatures, leading to phase change while employing the VLE-based PF model.

Acknowledgments

S. Yang gratefully acknowledges the support from the Office of Naval Research (ONR) grant under Award No. N00014-22-1-2287 under the supervision of project monitor Dr. Steven Martens, and the National Science Foundation (NSF) grant under Award No. CBET 2023932. The authors gratefully acknowledge the computing resources provided by the Minnesota Supercomputing Institute (MSI).

References

- [1] Yang, V., "Modeling of supercritical vaporization, mixing, and combustion processes in liquid-fueled propulsion systems," *Proceedings of the Combustion Institute*, Vol. 28, No. 1, 2000, pp. 925–942.
- [2] Van Konynenburg, P., and Scott, R., "Critical lines and phase equilibria in binary van der Waals mixtures," *Philosophical Transactions of the Royal Society of London. Series A, Mathematical and Physical Sciences*, Vol. 298, No. 1442, 1980, pp. 495–540.
- [3] Zhang, H., and Yang, S., "Numerical investigation of high-pressure transcritical shock-droplet interaction and mixing layer using VLE-based CFD accelerated by ISAT," *AIAA SCITECH 2023 Forum*, 2023, p. 1857.
- [4] Zhang, H., Yi, P., and Yang, S., "Multicomponent Effects on the Supercritical CO2 Systems: Mixture Critical Point and Phase Separation," *Flow, Turbulence and Combustion*, Vol. 109, No. 2, 2022, pp. 515–543.
- [5] Srinivasan, N., Zhang, H., and Yang, S., "A VLE-Based Reacting Flow Solver for High-Pressure Transcritical Two-Phase Combustion," *AIAA SCITECH 2023 Forum*, 2023, p. 1858.
- [6] Jain, S. S., "Accurate conservative phase-field method for simulation of two-phase flows," *Journal of Computational Physics*, Vol. 469, 2022, p. 111529.
- [7] Suresh, S. J., A Novel Diffuse-Interface Model and Numerical Methods for Compressible Turbulent Two-Phase Flows and Scalar Transport, Stanford University, 2021.
- [8] Chiu, P.-H., and Lin, Y.-T., "A conservative phase field method for solving incompressible two-phase flows," *Journal of Computational Physics*, Vol. 230, No. 1, 2011, pp. 185–204.

- [9] Michelsen, M. L., "Multiphase isenthalpic and isentropic flash algorithms," *Fluid phase equilibria*, Vol. 33, No. 1-2, 1987, pp. 13–27.
- [10] Rachford Jr, H., Rice, J., et al., "Procedure for use of electronic digital computers in calculating flash vaporization hydrocarbon equilibrium," *Journal of Petroleum Technology*, Vol. 4, No. 10, 1952, pp. 19–3.
- [11] Saha, S., and Carroll, J. J., "The isoenergetic-isochoric flash," Fluid phase equilibria, Vol. 138, No. 1-2, 1997, pp. 23-41.
- [12] Peng, D.-Y., and Robinson, D. B., "A new two-constant equation of state," *Industrial & Engineering Chemistry Fundamentals*, Vol. 15, No. 1, 1976, pp. 59–64.
- [13] Yi, P., Yang, S., Habchi, C., and Lugo, R., "A multicomponent real-fluid fully compressible four-equation model for two-phase flow with phase change," *Physics of Fluids*, Vol. 31, No. 2, 2019, p. 026102.
- [14] Wilson, G. M., "Vapor-liquid equilibrium. XI. A new expression for the excess free energy of mixing," *Journal of the American Chemical Society*, Vol. 86, No. 2, 1964, pp. 127–130.
- [15] Tudisco, P., and Menon, S., "Analytical framework for real-gas mixtures with phase-equilibrium thermodynamics," *The Journal of Supercritical Fluids*, Vol. 164, 2020, p. 104929.
- [16] Chung, T. H., Ajlan, M., Lee, L. L., and Starling, K. E., "Generalized multiparameter correlation for nonpolar and polar fluid transport properties," *Industrial & engineering chemistry research*, Vol. 27, No. 4, 1988, pp. 671–679.
- [17] Kee, R. J., Rupley, F. M., Meeks, E., and Miller, J. A., "CHEMKIN-III: A FORTRAN chemical kinetics package for the analysis of gas-phase chemical and plasma kinetics," Tech. rep., Sandia National Lab.(SNL-CA), Livermore, CA (United States), 1996.
- [18] Fuller, E. N., Schettler, P. D., and Giddings, J. C., "New method for prediction of binary gas-phase diffusion coefficients," Industrial & Engineering Chemistry, Vol. 58, No. 5, 1966, pp. 18–27.
- [19] Takahashi, S., "Preparation of a generalized chart for the diffusion coefficients of gases at high pressures," *Journal of Chemical Engineering of Japan*, Vol. 7, No. 6, 1975, pp. 417–420.
- [20] Foundation, T. O., OpenFOAM-6, www.openfoam.org, 2018.
- [21] Greenshields, C. J., Weller, H. G., Gasparini, L., and Reese, J. M., "Implementation of semi-discrete, non-staggered central schemes in a colocated, polyhedral, finite volume framework, for high-speed viscous flows," *International journal for numerical methods in fluids*, Vol. 63, No. 1, 2010, pp. 1–21.
- [22] Zhou, D., Zou, S., and Yang, S., "An OpenFOAM-based fully compressible reacting flow solver with detailed transport and chemistry for high-speed combustion simulations," AIAA Scitech 2020 Forum, 2020, p. 0872.
- [23] Zhang, H., Srinivasan, N., and Yang, S., "In Situ Adaptive Tabulation of Vapor-Liquid Equilibrium Solutions for Multi-Component High-Pressure Transcritical Flows with Phase Change," https://dx.doi.org/10.2139/ssrn.4534330, 2023.
- [24] Van Leer, B., "Towards the ultimate conservative difference scheme III. Upstream-centered finite-difference schemes for ideal compressible flow," *Journal of Computational Physics*, Vol. 23, No. 3, 1977, pp. 263–275.